JCI The Journal of Clinical Investigation

LXRβ/estrogen receptor-α signaling in lipid rafts preserves endothelial integrity

Tomonori Ishikawa, … , Philip W. Shaul, Michihisa Umetani

J Clin Invest. 2013;123(8):3488-3497. https://doi.org/10.1172/JCI66533.

Research Article **Vascular biology**

Liver X receptors (LXR) are stimulated by cholesterol-derived oxysterols and serve as transcription factors to regulate gene expression in response to alterations in cholesterol. In the present study, we investigated the role of LXRs in vascular endothelial cells (ECs) and discovered that LXRβ has nonnuclear function and stimulates EC migration by activating endothelial NOS (eNOS). This process is mediated by estrogen receptor-α (ERα). LXR activation promoted the direct binding of LXRβ to the ligand-binding domain of ERα and initiated an extranuclear signaling cascade that requires ERα Ser118 phosphorylation by PI3K/AKT. Further studies revealed that LXRβ and ERα are colocalized and functionally coupled in EC plasma membrane caveolae/lipid rafts. In isolated aortic rings, LXR activation of NOS caused relaxation, while in mice, LXR activation stimulated carotid artery reendothelialization via LXRβ- and ERα-dependent processes. These studies demonstrate that LXRβ has nonnuclear function in EC caveolae/lipid rafts that entails crosstalk with ERα, which promotes NO production and maintains endothelial monolayer integrity in vivo.

LXRβ/estrogen receptor-α signaling in lipid rafts preserves endothelial integrity

Tomonori Ishikawa,[1] Ivan S. Yuhanna,[1] Junko Umetani,[1] Wan-Ru Lee,[1] Kenneth S. Korach,[2] Philip W. Shaul,[1] and Michihisa Umetani[1,3]

[1]Division of Pulmonary and Vascular Biology, Department of Pediatrics, University of Texas Southwestern Medical Center, Dallas, Texas, USA. [2]Laboratory of Reproductive and Developmental Toxicology, National Institute of Environmental Health Sciences, Research Triangle Park, North Carolina, USA. [3]Department of Pharmacology, University of Texas Southwestern Medical Center, Dallas, Texas, USA.

Liver X receptors (LXR) are stimulated by cholesterol-derived oxysterols and serve as transcription factors to regulate gene expression in response to alterations in cholesterol. In the present study, we investigated the role of LXRs in vascular endothelial cells (ECs) and discovered that LXRβ has nonnuclear function and stimulates EC migration by activating endothelial NOS (eNOS). This process is mediated by estrogen receptor-α (ERα). LXR activation promoted the direct binding of LXRβ to the ligand-binding domain of ERα and initiated an extranuclear signaling cascade that requires ERα Ser118 phosphorylation by PI3K/AKT. Further studies revealed that LXRβ and ERα are colocalized and functionally coupled in EC plasma membrane caveolae/lipid rafts. In isolated aortic rings, LXR activation of NOS caused relaxation, while in mice, LXR activation stimulated carotid artery reendothelialization via LXRβ- and ERα-dependent processes. These studies demonstrate that LXRβ has nonnuclear function in EC caveolae/lipid rafts that entails crosstalk with ERα, which promotes NO production and maintains endothelial monolayer integrity in vivo.

Introduction

Liver X receptors (LXR) are members of the nuclear receptor superfamily that function as ligand-dependent transcription factors and play important roles in lipid metabolism (1–3). The 2 LXR isoforms, LXRα and LXRβ, share great similarity in protein structure and target genes, but they differ in tissue distribution. LXRα is primarily expressed in liver, kidney, intestine, adipose tissue, and macrophages, whereas LXRβ is ubiquitously expressed (4). Cholesterol-derived oxysterols such as 22(R)-hydroxycholesterol (22RHC) are endogenous ligands of LXR (5), and there are also synthetic LXR ligands that attenuate atherosclerosis development when administered to hypercholesterolemic mice (2, 6–8). The marked reductions in atherosclerosis in response to LXR agonists occur despite modest changes in plasma lipoprotein levels, suggesting that the underlying mechanism or mechanisms may involve direct effects on hematologic or vascular cell types of importance to atherogenesis. In macrophages, LXR upregulates a number of genes that promote reverse cholesterol transport to the liver (1, 9), and they inhibit macrophage inflammatory responses (3, 10). In vascular smooth muscle cells (VSMC), which also participate in atherogenesis and express LXR, LXR agonists attenuate mitogen-induced cell proliferation by inhibiting the expression of cell-cycle–regulating proteins (11). Whereas there are recognized functions of LXR in macrophages and VSMC, the potential roles of LXR in vascular endothelial cells (ECs), which are another cell type critically involved in atherogenesis (12), are unknown.

Similar to LXR, estrogen receptor-α and estrogen receptor-β (ERα and ERβ) are nuclear receptors that influence cardiovascular health and disease (13, 14). Estrogen treatment blunts atherosclerosis in mice, and the protection afforded by estrogen is not explained by changes in plasma lipoprotein levels (15, 16). Estrogen actions primarily via ERα promote reendothelialization following vascular injury, prevent neointima formation, and activate antiinflammatory responses (13). Along with their classical roles as transcriptional factors, both ERα and ERβ have nonnuclear function. These include the activation of kinases such as Akt in ECs, resulting in the stimulation of endothelial NOS (eNOS), increased production of the atheroprotective-signaling molecule NO, and the promotion of EC growth and migration (17–19). Nonnuclear actions of ERα and ERβ in ECs are mediated by receptor subpopulations that are associated with plasma membrane (PM) caveolae/lipid rafts (20, 21). There is recognized physiologic interplay between the LXR and ER ligand/receptor systems. LXR activation influences the synthesis and metabolism of estrogen (22, 23), estrogen causes attenuated expression of LXRα and its target genes in white adipose tissue (24), and estrogen also antagonizes LXR transcriptional activity in breast cancer cells (25). However, direct functional partnership between LXR and ER has not been previously observed in any biological context. In the current study, designed to elucidate the role of LXR in ECs, we discovered novel nonnuclear function of LXRβ that entails unique direct protein-protein interaction between LXRβ and ERα, and we show that these processes have important consequences on vascular NO production and the maintenance of endothelial monolayer integrity in vivo.

Results

LXRβ activation promotes EC migration via ERα and eNOS. To directly examine the role of LXR in EC, we evaluated cell migration in a scratch assay using the human EC line EA.hy926. A defined region of confluent ECs was removed with a cell scraper, cells were incubated under varying conditions for 20 hours, and the number of cells migrating past the wound edge was quantified. 17β-Estradiol (E_2, 10 nM) increased EC migration as previously reported

Authorship note: Tomonori Ishikawa and Ivan S. Yuhanna contributed equally to this work. Philip W. Shaul and Michihisa Umetani are co–senior authors.

Conflict of interest: Philip W. Shaul receives additional research support provided by Pfizer.

Citation for this article: *J Clin Invest.* 2013;123(8):3488–3497. doi:10.1172/JCI66533.

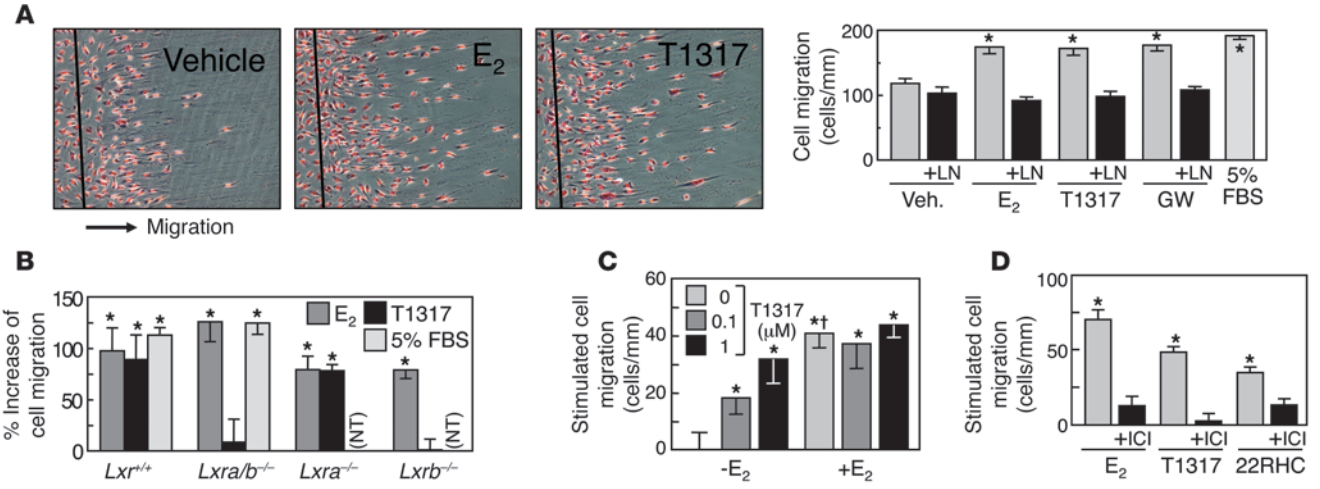

Figure 1

LXR activation promotes EC migration in a NOS-, LXRβ- and ER-dependent manner. EA.hy926 cells (**A**, **C**, and **D**) or isolated primary mouse EC (**B**) were grown to near-confluence, and a defined region was removed by a cell scraper. The cells were treated with vehicle control (Veh.), 10 nM E_2, 1 μM T1317, 1 μM GW, 10 μM 22RHC, or 5% FBS (as a positive control) in the absence or presence of 100 nM L-NAME (LN) (**A**) or 100 nM ICI (**D**) for 20 hours and stained with hematoxylin, and cells migrating past the wound edge (from left to right in **A**) were quantified. Original magnification, ×40. All graphs depict summary data (mean ± SEM, n = 3–4, $^*P < 0.05$ vs. vehicle control; $^\dagger P < 0.05$ vs. $-E_2$). NT, not tested.

(Figure 1A and refs. 19, 26), and the synthetic LXR agonists T0901317 (T1317) and GW3965 (GW) also promoted EC migration to degrees similar to those observed with 5% FBS. Evaluations of transcript abundance revealed that among the 2 known isoforms of LXR, LXRβ is the more abundant isoform in ECs (Supplemental Table 1; supplemental material available online with this article; doi:10.1172/JCI66533DS1), and the abundance of ERα and LXRβ proteins was not changed under the experimental conditions tested (Supplemental Figure 1A). Studies performed in the presence versus absence of hydroxyurea, which blocks cell division (27), demonstrated that the responses to E_2 and LXR agonists are indicative of cell migration occurring independently of the stimulation of cell growth (Supplemental Figure 1B). Recognizing the important role of eNOS in EC migration induced by stimuli such as VEGF and E_2 (28), the involvement of NOS in the actions of LXR agonists was assessed by NOS inhibition. The responses to E_2, T1317, and GW were all fully prevented by the nonselective NOS inhibitor N-nitro-L-arginine methyl ester (L-NAME) (Figure 1A). In contrast, neither iNOS- nor nNOS-specific inhibitors, 1400W and ARR17477, respectively, altered T1317-stimulated migration (Supplemental Figure 1C), indicating that the LXR-mediated processes are eNOS dependent. Primary ECs isolated from wild-type and LXR-null mice were then studied to determine whether the effect of the LXR agonist T1317 was LXR specific and to identify the operative receptor subtype(s). E_2 activated the migration of both *Lxr*$^{+/+}$ and *Lxra/b*$^{-/-}$ ECs (Figure 1B). In contrast, whereas T1317 promoted the migration of EC from *Lxr*$^{+/+}$ mice, there was no migration stimulated by T1317 in ECs from *Lxra/b*$^{-/-}$ mice. Furthermore, whereas the effect of T1317 on cell migration persisted in ECs from *Lxra*$^{-/-}$ mice, it was lost in ECs from *Lxrb*$^{-/-}$ mice, indicating that LXRβ is responsible for the EC migration stimulated by the LXR agonist. T1317 stimulated EC migration in a dose-dependent manner in the absence of E_2, and T1317 in the presence of a submaximal concentration of E_2 (10 nM) had neither an additive nor a synergistic effect (Figure 1C). Since the latter finding suggests that common mechanisms may mediate the responses to LXR and ER activation, potential functional linkage between the receptors was evaluated using the ER antagonist ICI 182,780 (ICI). ICI inhibited the EC migration stimulated by either E_2 or the LXR agonists T1317 and 22RHC (Figure 1D).

Next, we determined which ER isoform is responsible for the induction of migration by T1317 using the ERα- and ERβ-specific antagonists 1,3-bis(4-hydroxyphenyl)-4-methyl-5-[4-(2-piperidinylethoxy)phenol]-1H-pyrazole dihydrochloride (MPP) and 4-[2-phenyl-5,7-bis(trifluoromethyl) pyrazolo[1,5-a]pyrimidin-3-yl]phenol (PHTPP), respectively. T1317-stimulated migration was prevented by the ERα-specific antagonist MPP, but not by the ERβ-specific antagonist PHTPP (Supplemental Figure 2A). Furthermore, whereas E_2 and T1317 stimulated migration in control ECs previously transfected with scrambled siRNA sequence (scRNA) (Supplemental Figure 2B), the response was lost in ECs in which ERα protein abundance was reduced by siRNA (Supplemental Figure 2B). These cumulative results indicate that LXRβ activation promotes EC migration via ERα and eNOS.

LXR have nonnuclear action and activate eNOS and Akt via ER. In previous studies, we demonstrated that nonnuclear ERα signaling underlies estrogen-induced EC migration (19). Having found that LXRβ-mediated EC migration occurs via ERα, the possibility was raised that LXR have nonnuclear action in ECs that influences cell motility. We tested this by assessing rapid changes in the actin cytoskeleton in response to LXR agonist in the absence or presence of actinomycin D using phalloidin staining. Under control conditions, ECs exhibited diffuse distribution of actin and few if any stress fibers (Figure 2A). T1317 treatment (10 minutes) caused stress fiber formation, and the response was not altered by actinomycin D. Since the EC migration promoted by LXR activation is eNOS-dependent (Figure 1A), we next determined whether LXR acutely stimulate eNOS activity using bovine aortic EC (BAEC), in which rapid eNOS activation is readily quantified by measuring ^{14}C-L-arginine conversion to ^{14}C-L-citrulline in intact cells during

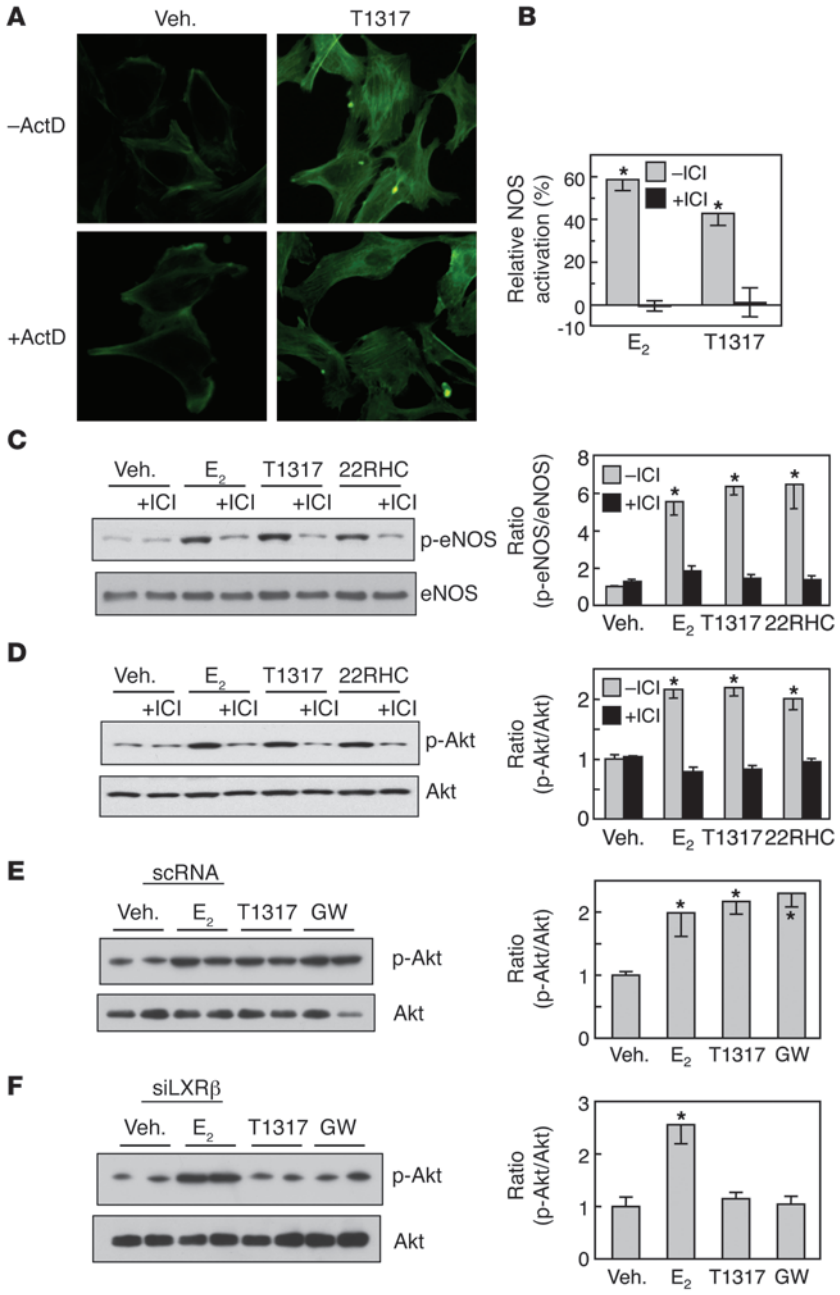

Figure 2
LXRβ has nonnuclear action in EC and activates eNOS and Akt via ER. (**A**) EA.hy926 cells were treated with vehicle or 1 μM T1317 for 10 minutes, with or without prior and concurrent treatment with 5 μg/ml actinomycin D, and changes in the actin cytoskeleton were visualized using Alexa Fluor 488 phalloidin. Representative images from 3 separate experiments. Original magnification, ×200. (**B**) eNOS activation in BAEC was tested during 15-minute incubations of intact cells with either 10 nM E_2 or 1 μM T1317, with or without 100 nM ICI added. Values are mean ± SEM, $n = 3–4$; $^*P < 0.05$ vs. vehicle control. (**C** and **D**) ECs were treated with 10 nM E_2, 1 μM T1317, or 10 μM 22RHC with or without 100 nM ICI for 20 minutes. Phosphorylated eNOS (Ser1177) and total eNOS (**C**), or phosphorylated Akt (Ser473) and total Akt (**D**) were then detected by immunoblot analysis, and the ratios of phospho-eNOS to total eNOS (**C**) and phospho-Akt to total Akt (**D**) were calculated (mean ± SEM, $n = 3$, $^*P < 0.05$ vs. vehicle control). (**E** and **F**) scRNA (**E**) or siRNA against LXRβ (siLXRβ) (**F**) were introduced into BAEC, and 48 hours later, the cells were treated with 10 nM E_2, 1 μM T1317, or 1 μM GW for 20 minutes. The abundance of phospho-Akt relative to total Akt was determined by immunoblotting (mean ± SEM, $n = 3$, $^*P < 0.05$ vs. vehicle control). In **C**–**F**, representative blots from 3 separate experiments are shown.

15-minute incubations (19). Both E_2 and T1317 activated eNOS, and both responses were fully abolished by ICI (Figure 2B). eNOS activation by ERα is mediated by the phosphorylation of the serine residue at amino acid 1177 (Ser1177) of eNOS by Akt (18). E_2 and the LXR agonists T1317 and 22RHC caused increases in eNOS Ser1177 phosphorylation, and the promotion of phosphorylation by all agents was inhibited by ER antagonism with ICI (Figure 2C). E_2 and the LXR agonists also induced comparable phosphorylation of Akt at Ser473 (Figure 2D), the increase was inhibited by ICI, and in studies of T1317 activation of Akt, it was observed as early as 5 minutes after agonist exposure (Supplemental Figure 3).

To then determine whether LXRβ is required for the effect of LXR agonists on Akt, siRNA against LXRβ was introduced into ECs. The siRNA targeting LXRβ markedly decreased LXRβ protein abundance, but not ERα expression in ECs (Supplemental Figure 4). Whereas E_2, T1317, and GW induced equal Akt phosphorylation in control cells (Figure 2E), the knockdown of LXRβ fully prevented Akt phosphorylation in response to T1317 and GW, but not in response to E_2 (Figure 2F). Taken together, these results indicate that LXRβ has nonnuclear action in EC, that LXRβ activates eNOS by stimulating its phosphorylation by Akt, and that these processes are entirely ER dependent. It is notable that, in contrast, nonnuclear ER signaling is not dependent on LXRβ.

LXRβ interacts directly with the ligand-binding domain of ERα. To investigate potential functional interaction between LXRβ and ERα of consequence to nonnuclear LXRβ signaling in ECs, we first performed coimmunoprecipitation experiments using EC whole-cell lysates and an anti-ERα antibody. LXRβ was coimmu-

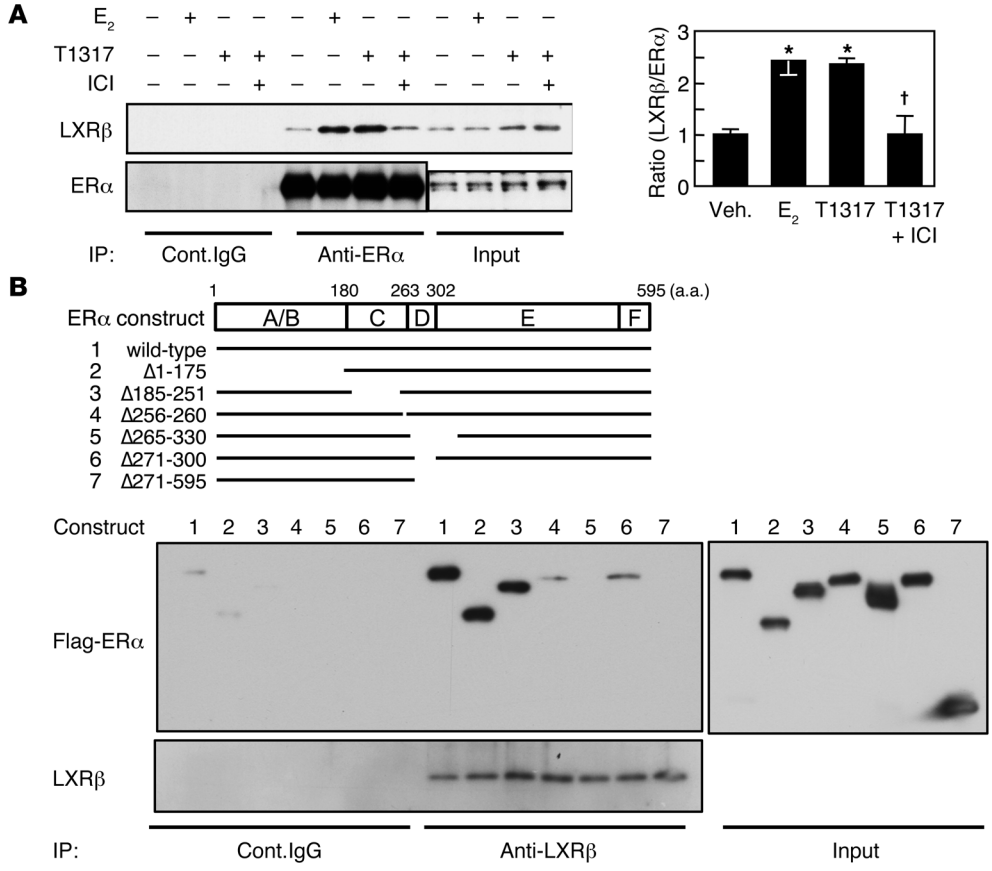

Figure 3

LXRβ and ERα interact directly via the ligand-binding domain of ERα. (**A**) EA.hy926 cells were treated with vehicle, 10 nM E_2, 1 μM T1317, or T1317 plus 100 nM ICI for 20 minutes, and cell lysates were prepared for immunoprecipitation with control IgG (cont. IgG) or anti-ERα antibody. Immunoprecipitated proteins were detected by immunoblotting with anti-LXRβ or anti-ERα antibodies, and the ratio of immunoprecipitated LXRβ to ERα proteins against vehicle control was calculated (mean ± SEM, $n = 3$, $^*P < 0.05$ vs. vehicle control, $^\dagger P < 0.05$ vs. T1317 alone). For the ERα immunoblot, the lanes were run on the same gel but were noncontiguous. (**B**) In vitro coimmunoprecipitation assays were performed using recombinant wild-type Flag-ERα or deletion mutant proteins and LXRβ protein. Linear depiction of the ERα constructs tested (numbered 1–7) is provided in the upper panel. The proteins were incubated with 1 μM T1317 for 2 hours at 4°C, and immunoprecipitation was performed with control IgG or anti-LXRβ antibody. Immunoprecipitated proteins were separated by SDS-PAGE and detected by immunoblot analysis with anti-Flag or anti-LXRβ antibodies. Results shown in **A** and **B** were confirmed in at least 3 independent experiments.

noprecipitated with ERα, the amount of LXRβ coimmunoprecipitated with ERα was increased by EC treatment with T1317 or E_2, and the increase in interaction caused by T1317 was inhibited by ICI (Figure 3A). To determine whether the LXRβ-ERα interaction is a direct protein-protein interaction, coimmunoprecipitation assays were performed using purified, recombinant Flag-tagged ERα, recombinant LXRβ, and anti-LXRβ antibody. Full-length, wild-type Flag-ERα was pulled down with anti-LXRβ antibody (Figure 3B, construct 1), and in separate experiments the interaction between LXRβ and ERα was increased by the addition of either T1317 or E_2 (Supplemental Figure 5A). In addition, it was found that LXRβ is capable of interaction with ERβ, but modulation by ligand was not observed (Supplemental Figure 5B).

To determine which domain of ERα is involved in the direct protein-protein interaction between LXRβ and ERα, recombinant Flag-tagged deletion mutants of ERα were used in the coimmunoprecipitation assay (Figure 3B). Deletion mutants lacking the N-terminal 175 residues of ERα (construct 2) or portions of the DNA-binding domain or C domain of ERα (construct 3 and 4) displayed direct interaction with LXRβ similar to wild-type, full-length receptor. Mutants lacking the N-terminal portion of the ligand-binding domain or E domain (construct 5 and 7) did not display interaction, whereas a mutant lacking amino acids 271–300 (construct 6) showed interaction. These cumulative observations indicate that LXRβ and ERα interact in ECs, that there is direct protein-protein interaction between the receptors that involves amino acids 300–330 within the ligand-binding domain of ERα, and that the interaction is dynamically regulated by ligand binding to either receptor.

LXRβ is functionally coupled to ERα in EC caveolae/lipid rafts. Because nonnuclear ERα functions in ECs are mediated by receptors localized to PM caveolae/lipid rafts (28), we next determined by subfractionation whether a subpopulation of LXRβ is colocalized with ERα in EC PM caveolae/lipid rafts. We employed our established caveolae membrane isolation method, which yields a fraction that is free of nuclear proteins (20, 29). Both ERα and LXRβ proteins were associated with the PM fraction and also with the caveolae membranes (Figure 4A), and as expected, both receptor proteins were abundant in the nuclear fraction. Mirroring the LXRβ-ERα interaction observed in EC whole-cell lysates (Figure 3A), their interaction was also demonstrated in nuclear and PM fractions by coimmunoprecipitation using anti-ERα antibody (Figure 4B). More importantly, in isolated caveolae membranes, T1317 activated eNOS, and the activation was fully prevented by ER antagonism with ICI (Figure 4C). In addition, Akt activation stimulated by T1317 in intact ECs was prevented by cell treatment with methyl-β-cyclodextrin, which destroys caveolae structure (30), providing further evidence that the localization of LXR in caveolae/lipid rafts is required for nonnuclear signaling by the receptor (Supplemental Figure 6). Thus, there is a subpopulation of LXRβ colocalized with ERα in EC caveolae/lipid rafts, and in the microdomain, there is functional coupling of LXRβ with ERα that enables LXRβ to modulate kinase-dependent processes.

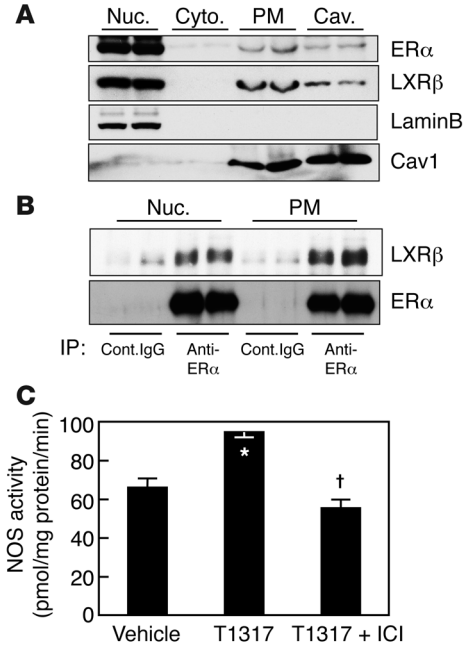

Figure 4
LXRβ is colocalized and functionally coupled to ERα in EC caveolae/lipid rafts. (**A**) ERα and LXRβ abundance in BAEC nuclear (Nuc), cytoplasmic (Cyto), PM and caveolae/lipid raft (Cav) fractions were evaluated by immunoblot analysis. Lamin B and caveolin-1 (Cav1) proteins served as markers of nuclear and caveolae/lipid raft fractions, respectively. (**B**) BAEC nuclear and PM proteins isolated in **A** were subjected to immunoprecipitation using control IgG or anti-ERα antibody in the presence of 1 μM T1317 for 1 hour, followed by immunoblot analysis with anti-LXRβ or anti-ERα antibodies. In **A** and **B**, protein distributions were assessed in 2 parallel samples. (**C**) eNOS activity in the caveolae/lipid raft fraction of BAEC was quantified during 60-minute incubations with vehicle, 1 μM T1317, or T1317 plus 100 nM ICI. Values are mean ± SEM, $n = 3$, $^*P < 0.05$ vs. vehicle control; $^\dagger P < 0.05$ vs. T1317 alone. Findings were confirmed in 2 independent experiments.

Nonnuclear LXRβ signaling requires PI3K-Akt–dependent ERα Ser118 phosphorylation. In the absence of estrogen, peptide growth factors such as EGF and IGF-1 cause the phosphorylation of ERα at Ser118. This process is mediated by MAP kinase, and it enhances the binding of the receptor to p160 coactivators (31, 32). Since we have discovered that LXR has nonnuclear function in ECs mediated by ERα in the absence of estrogen, we determined whether LXR activation causes the phosphorylation of ERα. Either E_2 or T1317 treatment for 20 minutes resulted in an increase in ERα Ser118 phosphorylation, and ICI inhibited T1317-induced phosphorylation (Figure 5A). To identify the signaling mechanisms that underlie ERα Ser118 phosphorylation by LXR, pharmacologic inhibitors of kinases known to be required for ERα phosphorylation were used (33). ERα phosphorylation induced by the LXR agonist GW was attenuated by the PI3K inhibitor LY294002 and by the Akt inhibitor Akti-1/2, but not by the MEK1/2 inhibitor PD0325901 (Figure 5B). Thus, PI3K and Akt are required for ERα Ser118 phosphorylation in response to LXR activation. LY294002 and Akti-1/2 also inhibited Akt Ser473 phosphorylation activated by LXR agonist (Figure 5C). In parallel studies, PI3K inhibition by LY294002 blunted both E_2- and T1317-induced activation of Akt Ser473 phosphorylation and EC migration (Supplemental Figure 7).

To further delineate whether ERα Ser118 phosphorylation is necessary for LXR nonnuclear signaling, we tested LXR agonist activation of Akt phosphorylation in HEK293 cells that have endogenous LXRβ but not ERα (Supplemental Figure 8A). E_2, T1317, and GW failed to induce Akt phosphorylation in the parental ERα-negative HEK293 cells (Figure 5D). In contrast, in HEK293 cells expressing ERα, Akt phosphorylation was activated by E_2 or the LXR agonists, and the activation by all 3 compounds was inhibited by ICI (Figure 5E). However, E_2 and the LXR agonists failed to activate Akt phosphorylation in cells expressing a mutant form of ERα in which Ser118 was mutated to alanine (ERα S118A; Figure 5F and Supplemental Figure 8A). Using immunoblotting of the PM-associated receptors, we further determined that the failure of Akt phosphorylation in response to E_2 and LXR agonists in ERα Ser118A-expressing cells was not due to altered PM localization of either endogenous LXRβ or the mutant ERα protein (Supplemental Figure 8B). Furthermore, the overexpression of ERα Ser118A in ECs had a dominant negative effect, completely preventing the stimulation of EC migration by either E_2 or T1317 (Figure 5G). Taken together, these results demonstrate that ERα Ser118 phosphorylation by PI3K-Akt is required for nonnuclear signaling and resulting cell migration provoked by LXRβ.

LXR activation relaxes precontracted aortic rings via NOS stimulation. To translate the observations regarding LXR coupling to eNOS in cultured ECs to the function of the receptor in intact endothelium, tensiometry was performed using isolated rings of rat aorta, in which NOS activation by ER and resulting effects on vascular tension can be quantified (26, 34). Aortas were incubated with E_2 or T1317 for 24 hours, and contraction induced by 100 nM phenylephrine (PE) was measured. The stimulation of contraction by PE was blunted by treatment with E_2 or T1317 (Figure 6, A and B, and Supplemental Figure 9). We confirmed that the endothelium was intact in all samples by evaluating relaxation in response to acetylcholine at the end of the assay. The inhibition of PE-induced contraction by T1317 was dose dependent (Supplemental Figure 9), and the vasodilating effects of both E_2 and T1317 were not observed in the presence of the NOS antagonist NG-methyl-L-arginine (L-NNA), indicating that they are NOS dependent. Importantly, the effects of E_2 and T1317 on aortic contraction were not related to changes in eNOS protein abundance (Figure 6C). These findings indicate that LXR activation causes vascular relaxation via the stimulation of NOS activity in intact endothelium.

LXRβ activation promotes reendothelialization via ERα. To determine how LXR regulate vascular endothelium in vivo, we studied carotid artery reendothelialization after perivascular electric injury in mice, which is an established model in which nonnuclear ERα activation promotes endothelial repair (19). Male mice were treated with vehicle or T1317 for 3 days, and carotid artery endothelium was denuded by perivascular electric injury. The mice subsequently received treatment for 4 additional days, and the amount of remaining denudation 4 days after injury was visualized using Evans blue dye. Figure 7A shows representative images of the carotid artery intimal surface, and summary findings are given in Figure 7B. In *Lxra/b*$^{+/+}$ and *Lxra*$^{-/-}$ mice, markedly more reendothelialization occurred with T1317 versus vehicle treatment, as indicated by the smaller area of remaining denudation. In contrast, the promotion of reendothelialization by T1317 did not occur in *Lxra/b*$^{-/-}$ or in *Lxrb*$^{-/-}$ mice. We next determined whether LXRβ-mediated reendothelialization requires ERα. The effect of the LXR agonist T1317 on reendothelial-

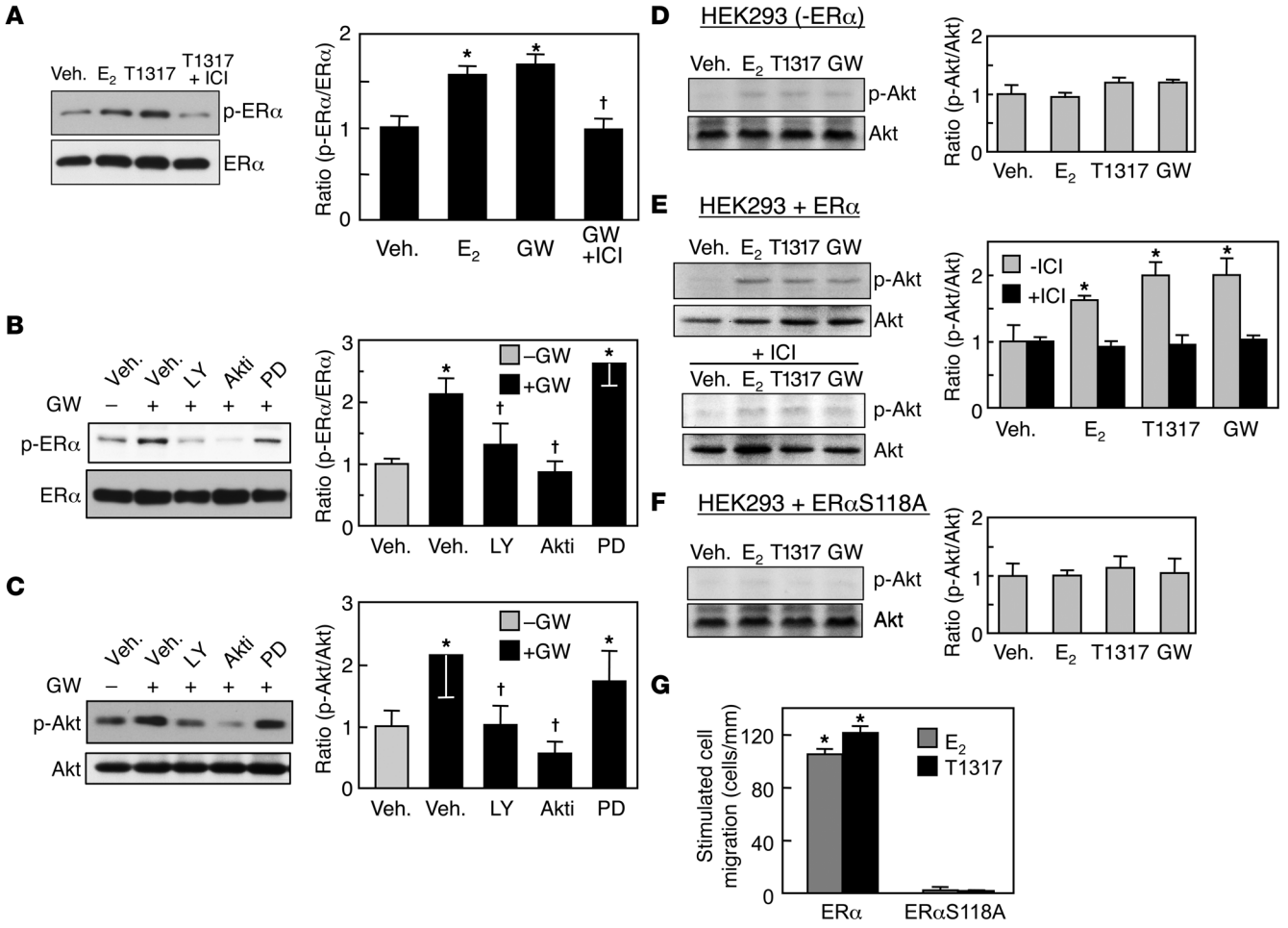

Figure 5

LXR activation causes EC migration via PI3K–Akt-dependent ERα S118 phosphorylation. (**A**) EC were treated with vehicle (Veh.), 10 nM E_2, 1 μM T1317, or T1317 plus 100 nM ICI, and protein abundance of phosphorylated ERα (Ser118) and total ERα were detected by immunoblot analysis (mean ± SEM, $n = 3$, *$P < 0.05$ vs. vehicle control; †$P < 0.05$ vs. GW alone). (**B** and **C**) ECs were treated with vehicle, 10 μM LY294002 (LY), 10 μM Akti-1/2, or 25 nM PD 0325901 (PD) for 1 hour, followed by vehicle or 1 μM GW treatment for 20 minutes. Cells were harvested and phosphorylated ERα (Ser118), total ERα, phosphorylated Akt (Ser473), and total Akt were detected (mean ± SEM, $n = 3$, *$P < 0.05$ vs. vehicle control; †$P < 0.05$ vs. GW alone). (**D**–**F**) Parental HEK293 cells (**D**), or HEK293 cells stably transfected with wild-type ERα (**E**) or ERα S118A (**F**) were treated with vehicle, 10 nM E_2, 1 μM T1317, or 1 μM GW for 20 minutes, and phosphorylated Akt (Ser473) and total Akt were detected by immunoblot analysis (mean ± SEM, $n = 3$, *$P < 0.05$ vs. vehicle control). In **A**–**F**, representative immunoblots from 3 separate experiments are shown; summary data are shown for phosphorylated ERα and Akt protein abundance normalized to total ERα and Akt abundance, respectively. (**G**) BAEC were transfected with ERα or ERα S118A expression plasmids, and cell migration in response to vehicle, 10 nM E_2, or 1 μM T1317 treatment for 20 hours was evaluated (mean ± SEM, $n = 3$–4, *$P < 0.05$ vs. vehicle control).

ization was compared in *Era*$^{+/+}$ male mice treated with vehicle versus the ER antagonist ICI for 3 days prior to injury and for 4 days after injury. In *Era*$^{+/+}$ mice, T1317 promoted reendothelialization, and this was fully prevented by concomitant treatment with ICI (Figure 7, C and D). Furthermore, T1317-induced reendothelialization was absent in *Era*$^{-/-}$ mice. These findings mirror the observation regarding ERα-dependent, LXRβ-induced activation of migration by cultured ECs (Figure 1). Thus, LXRβ activation promotes reendothelialization in vivo, and the process requires ERα.

Discussion

In the current study, we investigated the role of LXR in the regulation of EC function and discovered a pathway by which nonnuclear actions of LXRβ promote EC migration. Using complementary EC and reconstitution cell-culture models as well as in vitro protein-protein interaction assays, we found that LXRβ interacts directly with ERα via the ligand-binding domain of ERα, that upon activation by its ligands, LXRβ has increased interaction with ERα and causes ERα Ser118 phosphorylation through PI3K-Akt, and that the phosphorylation of ERα Ser118 is required for resulting eNOS-dependent stimulation of EC migration.

We and others have previously demonstrated that a PM-associated subpopulation of ER causes potent activation of EC growth and migration and the inhibition of apoptosis in EC (17, 35). These processes are mediated by ER in caveolae/lipid rafts that are coupled to multiple signaling molecules including Src, PI3K, and Akt, and thereby also to eNOS (20, 28). In the present study, we provide what we believe is the first evidence that a subpopu-

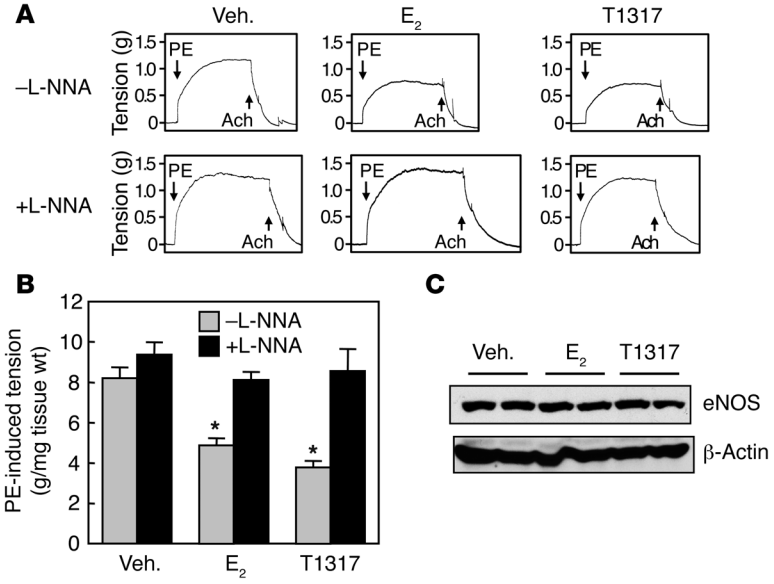

Figure 6
LXR activation stimulates NOS in intact aortic endothelium. (**A**) PE-stimulated contraction was measured in rat aortic rings previously incubated with vehicle, 10 nM E_2, or 1 μM T1317 for 24 hours. L-NNA (100 μM) was added to selected rings 20 minutes before PE stimulation. After tension reached maximum level, 10 μM acetylcholine was added to evaluate endothelium-dependent, NOS-dependent relaxation. (**B**) Summary data for aortic tension are expressed as gram tension per tissue wet weight (mean ± SEM; n = 8–12 per group; *$P < 0.05$ vs. vehicle control). (**C**) Aorta samples incubated with compound for 24 hours were homogenized, and protein abundance of eNOS and β-actin was determined by immunoblotting. Each lane represents individual aorta samples.

lation of LXRβ is associated with caveolae/lipid rafts on the EC PM and that through partnership with ERα in caveolae, LXRβ is operative in nonnuclear signaling of consequence to EC behavior. The biochemical approach used for the caveolae/lipid raft fractionation is a well-established method, and we and others have confirmed that the caveolae membranes obtained are not contaminated by proteins from the nucleus (20, 29), where LXR is abundant. Importantly, we demonstrate functional coupling of LXR with ER that results in eNOS activation in isolated caveolae/lipid rafts. Further evidence of LXR function on the PM was obtained by the observation that LXR agonist activation of Akt in intact ECs was prevented by the disruption of caveolae architecture with cyclodextrin. Interestingly, in VSMCs, LXR activation alters angiotensin II–induced phosphorylation of Erk and also the phosphorylation of the transcription factor SP1 (36). Thus, nonnuclear signaling by LXR may serve important functions in additional cell types besides ECs.

Our work also indicates that LXRβ interacts directly with ERα and that the interaction is increased by LXR agonist or by E_2. It has been reported that LXR directly binds to AP1 (37), which is a well-known molecular and functional partner of ERα. However, we believe the current findings are the first to demonstrate direct interaction between LXR and a steroid hormone receptor. We further delineated that the interaction involves the N terminus of the ERα ligand–binding domain and that the ER antagonist ICI fully inhibits the promotion of LXRβ-ERα interaction by LXR agonist. Since we previously demonstrated that structurally different ER ligands induce distinct conformational changes in ERα (38), the latter finding suggests that the dynamic interaction between LXRβ and ERα is strongly influenced by the tertiary structures of the 2 receptor proteins.

Multiple steroid and nonsteroid nuclear receptors such as ER, progesterone receptor, androgen receptor, retinoic acid receptor, retinoid X receptor, and vitamin D receptor are activated in a ligand-independent manner by phosphorylation (33, 39, 40). ERα has a protein-protein interaction with the IGF-1 receptor and is phosphorylated at Ser118 by IGF-1 through MAPK in the absence of E_2 (31), and this process influences the transcriptional activity of ERα and contributes to the development of ER-positive cancer cell resistance to endocrine therapy (33). Our discovery that ERα Ser118 phosphorylation is required for either E_2 or LXR agonist to invoke Akt activation is the first demonstration, to our knowledge, that Ser118 phosphorylation promotes the nonnuclear function of ERα. LXR modulation of ERα Ser118 phosphorylation differs from the process by which IGF-1 does so because MAPK is not required. In addition, it is notable that Akt participates both upstream and downstream of ERα in this newly identified LXRβ nonnuclear signaling cascade. Recognizing that multiple isoforms of Akt are expressed in EC and that the Akt isoforms serve distinct functions (41–43), one possibility worthy of future study is that different Akt isoforms participate proximal versus distal to ERα.

Our observations regarding mechanistic linkage between LXRβ and ERα and the resulting promotion of both NO production by the endothelium of intact arteries and endothelial monolayer integrity in vivo have potentially important implications for cardiovascular health and disease. NO is a potent atheroprotective molecule via numerous mechanisms, and NO deficiency contributes to the earliest process in atherogenesis (28, 44). The disruption of the endothelial monolayer plays an integral role in the initiation of both restenosis and atherosclerosis (12). It perturbs the ability of the endothelium to modulate local hemostasis and thrombolysis, and in the absence of the tempering influence of the endothelium, VSMC proliferate and produce extracellular matrix proteins, resulting in the formation of neointima or atherosclerotic lesions (12). Consistent with our discovery that LXRβ partnership with ERα avidly promote NO production and endothelial monolayer integrity through processes that are independent of LXRα, previous studies have shown that LXRβ activation attenuates atherosclerosis in the absence of LXRα (45, 46). Interestingly, it has been observed that the atheroprotection afforded by LXR agonists is greater in male versus female mice. Since female mice (6) are less prone to atherosclerosis than males due to estrogen- and ERα-mediated processes (16), the decreased atheroprotection provided by LXR agonists in females versus males may be consistent with our finding that LXR and ER modify EC behavior through common mechanisms. Thus, our

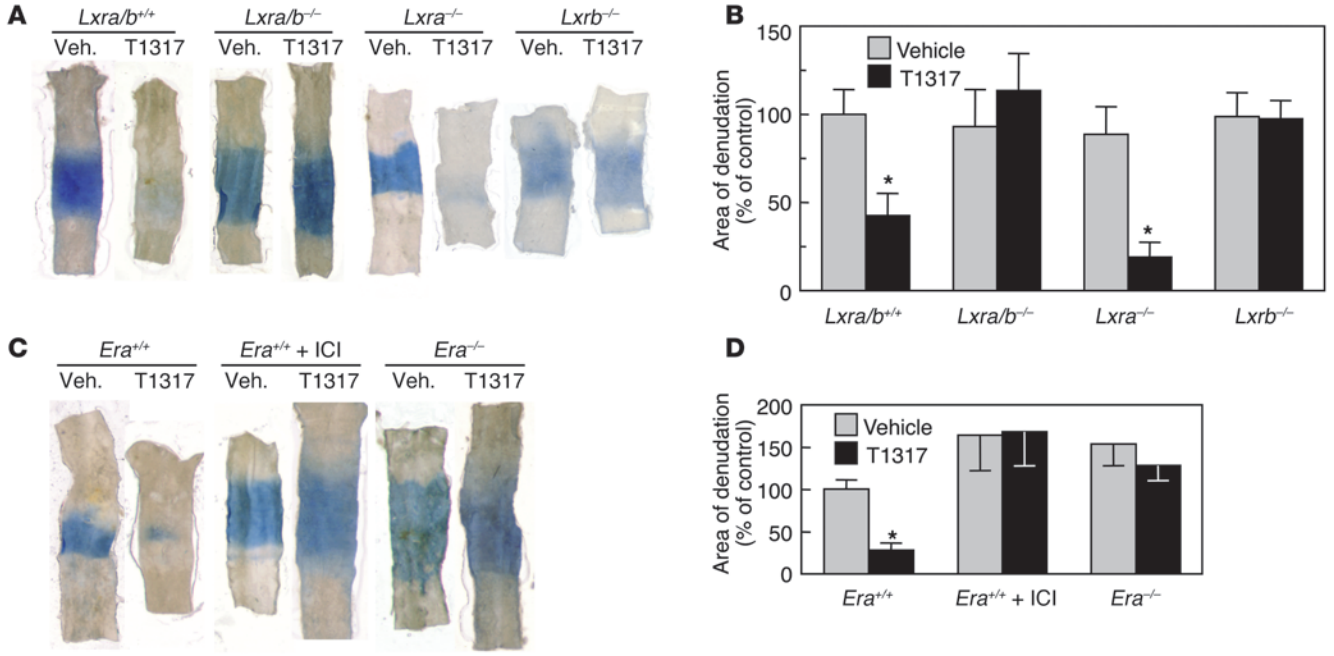

Figure 7

LXRβ activation promotes reendothelialization in mice in an ERα–dependent manner. (**A** and **B**) Reendothelialization of the carotid artery was evaluated in male *Lxra/b*$^{+/+}$, *Lxra/b*$^{-/-}$, *Lxra*$^{-/-}$, and *Lxrb*$^{-/-}$ mice fed a diet containing either vehicle or T1317. (**C** and **D**) Reendothelialization experiments were performed in *Era*$^{+/+}$ mice, in *Era*$^{+/+}$ mice treated with ICI, and in *Era*$^{-/-}$ mice fed a diet containing either vehicle or T1317. Four days after perivascular electric injury, mice were injected with Evans blue dye and the area of intimal surface dye incorporation was quantified. (**A** and **C**) Intimal surfaces of representative carotid arteries are shown. (**B** and **D**) Remaining area of denudation (arbitrary pixel units of blue stain) was quantified, and summary data are expressed as percentage of vehicle-treated *Lxra/b*$^{+/+}$ or *Era*$^{+/+}$ controls (mean ± SEM; n = 6–7 per group; $^*P < 0.05$ vs. vehicle treatment).

discovery of the capacity of LXRβ to beneficially affect both NO production and endothelial repair via coupling with ERα may explain certain prior observations regarding the role of LXRβ in the modulation of vascular health and disease. A limit of the current work is that the discrete role of EC LXRβ in protection from atherosclerosis and other vascular disorders has not been directly interrogated by cell-specific gene silencing in vivo. However, based on the new functional pathway that we report, future studies of this nature are warranted.

Using complementary cell culture and in vivo models and both genetic and pharmacologic manipulation, we have identified an unanticipated nonnuclear function of LXRβ in ECs and show that this entails unique crosstalk between LXRβ and ERα, with important consequences on both NO production and endothelial monolayer integrity. Further work targeting endothelial LXRβ-mediated processes may lead to new prophylactic or therapeutic approaches to restenosis, atherosclerosis, and other vascular diseases.

Methods

Materials. T1317 and 1400W were purchased from Cayman Chemical Co. ICI, MPP, and PHTPP were purchased from Tocris. LY294002, Akti-1/2, and PD0325901 were purchased from EMD Millipore. L-NAME, E_2, GW, 22RHC, hydroxyurea, ARR17477, methyl-β-cyclodextrin, and L-NNA were purchased from Sigma-Aldrich. Anti-phosphorylated eNOS (Ser1177), anti-total eNOS, anti-phosphorylated Akt (Ser473), anti-total Akt, anti–caveolin-1, and anti-phosphorylated ERα (Ser118) antibodies were purchased from Cell Signaling. Anti-total ERα, anti–β-actin, anti-ERβ, and anti–lamin B antibodies were purchased from Santa Cruz Biotechnology Inc. Anti-LXRβ and anti-Flag antibodies were purchased from Perseus Proteomics and Roche Diagnostics, respectively.

RT-qPCR. Evaluations of transcript abundance were performed using RT-qPCR as described in the Supplemental Methods and Supplemental Table 2.

EC migration. Migration studies were performed as described (26). Briefly, EA.hy926 cells were plated in 1% dextran-charcoal–stripped FBS on 6-well plates and grown to near confluence, cells in half the well were removed with a cell scraper, the remaining cells were washed with PBS and treatments were added, and 20 hours later, they were stained with hematoxylin. To quantify cell migration, we counted cells that had migrated past the wound edge per mm wound length. In additional experiments, ECs were obtained from *Lxra/b*$^{+/+}$ or *Lxra/b*$^{-/-}$ mice as previously described (47). The cells were used within 3 passages. When multiple reagents were used, cells were treated with them concurrently. EC experiments employing siRNA for gene silencing or involving gene introduction were performed using BAEC in which these manipulations are readily accomplished by transfection using Lipofectamine 2000 (26).

Actin immunofluorescence. EA.hy926 cells were plated on 8-well chamber slides (Lab-Tek) in 5% dextran-charcoal–stripped FBS. The following day the cells were treated with vehicle or T1317 for 10 minutes, fixed in 3% paraformaldehyde in PBS for 10 minutes, washed 3 times with PBS, stained with Alexa Fluor 488 phalloidin (Molecular Probes), and viewed by fluorescent microscopy. The requirement for gene transcription in LXR-induced changes in the actin cytoskeleton was tested by adding actinomycin D (5 μg/ml).

Immunoblot analyses. eNOS and Akt phosphorylation were detected by immunoblot analysis with anti–phospho-eNOS (Ser1177) and anti–phospho-Akt (Ser473) antibodies, respectively, and results were nor-

malized for total eNOS and Akt abundance detected by anti-eNOS and anti-Akt antibodies, respectively. Reconstitution experiments for the study of ERα phosphorylation, which entailed comparisons of wild-type and mutant forms of ERα, were performed in HEK293 cells. These were chosen because HEK293 cells express endogenous LXRβ, but lack endogenous ERα. Wild-type ERα or ERα S118A expression plasmid was transfected into HEK293 cells using FuGENE6 (Roche Diagnostics), stably transfected cells were isolated by G418 selection, and Akt Ser473 phosphorylation in response to E_2 or LXR agonist was evaluated. ERα phosphorylation was detected by immunoblot analysis with anti–phospho-ERα (Ser118) antibody, and results were normalized for total ERα abundance detected by anti-ERα antibody.

To evaluate receptor localization in the nucleus and in PM and caveolae/lipid rafts in BAEC, nuclear fractions were prepared and PM and caveolae membranes were isolated using Percoll–density dependent separation as described (20), and 25 μg of protein per sample was loaded per lane; immunoblotting was performed for ERα and LXRβ. Lamin B and caveolin-1 distribution were evaluated to confirm a lack of contamination of the caveolae/lipid raft fraction with nuclear proteins. Additional caveolae membranes were isolated and subjected to assessments of eNOS activation.

Coimmunoprecipitation assays. In coimmunoprecipitation experiments testing protein interaction in ECs, the cells were treated with vehicle, T1317 (1 μM), or E_2 (10 nM) for 20 minutes; immunoprecipitation was performed with control IgG, anti-ERα, or anti-LXRβ antibodies; and coimmunoprecipitated proteins were detected by immunoblotting. To study direct protein-protein interaction, in vitro–translated LXRβ and 1 μg of either purified, recombinant Flag-tagged ERα or intact ERβ (Invitrogen) was incubated with compounds for 2 hours at 4°C, followed by immunoprecipitation. Flag-tagged wild-type ERα and deletion mutant proteins were generated from Sf9 cells infected with baculovirus encoding human ERα constructs as described (48). Immunoprecipitated proteins were detected by immunoblotting with anti-Flag, anti-LXRβ, and anti-ERβ antibodies.

eNOS activation. eNOS activity was assessed by measuring the conversion of [^{14}C]L-arginine (Amersham) to [^{14}C]L-citrulline in intact BAEC during 15-minute incubations (26) or in isolated EC caveolae membranes over 60 minutes (20).

Aortic tension measurement. Aortic tension in rings of rat thoracic aorta was measured as described before (26). Aortic rings were incubated at 37°C, 5% CO_2, 95% O_2-gassed phenol red–free DMEM with vehicle or compounds for 24 hours, then transferred to organ chambers, and 100 nM PE-stimulated contraction was measured. For L-NNA treatment, vehicle or 100 μM L-NNA was added to the rings 20 minutes before PE stimulation. Endothelium-dependent responses were confirmed by reactivity to 10 μM acetylcholine.

Carotid artery reendothelialization. Mouse carotid artery reendothelialization after perivascular electric injury was performed as described (26). Briefly, the superior portion of the left carotid artery was subjected to electric current along 4 mm of artery length using bipolar forceps. This results in endothelial denudation with minimal effect on the medial layer (49). The area of remaining denudation 4 days after injury was determined by injection of Evans blue dye into the left ventricle, which is incorporated in the denuded region, and quantification of the dye-stained area by blinded image analysis. Endothelial denudation and recovery after injury in this model has been confirmed by immunohistochemistry for von Willebrand factor (50). Studies were performed in *Lxra/b*$^{+/+}$, *Lxra*$^{-/-}$, *Lxrb*$^{-/-}$, and *Lxra/b*$^{-/-}$ mice, or in *Era*$^{+/+}$ and *Era*$^{-/-}$ mice (51–53), which were housed in a temperature-controlled environment with 12-hour light/12-hour dark cycles. Age-matched (16 to 20 weeks old) male mice were fed ad libitum standard chow powdered diet supplemented with T1317 (50 mg/kg body weight) or vehicle (0.9% carboxy methyl cellulose, 9% PEG 400, and 0.05% Tween 80) from 3 days before vascular injury through the duration of the experiments. For ICI treatment, animals were injected subcutaneously with 100 μg/mouse of ICI or vehicle daily from 3 days before the injury through the duration of the experiments.

Statistics. Results are presented as mean ± SEM, and differences between groups were assessed by 1-way ANOVA followed by the Neuman-Keuls procedure. $P < 0.05$ was considered statistically significant.

Study approval. All animal experiments were approved by the UT Southwestern Medical Center Institution Animal Care and Research Advisory Committee.

Acknowledgments

The authors thank K. Chambliss, C. Mineo, K. Kamm, K. Luby-Phelps, and K. Rothberg for help on experiments; C.-J. Edgell for providing EA.hy926 cells; D. Mangelsdorf and S. Kliewer for critical review of the manuscript; and members of the Shaul and Mango/Kliewer labs for helpful suggestions. This work was supported by grants from the American Heart Association (0865158F to M. Umetani), the NIH (HL087564 to P.W. Shaul), and the Lowe Foundation (to P.W. Shaul).

Received for publication August 24, 2012, and accepted in revised form May 9, 2013.

Address correspondence to: Michihisa Umetani, Division of Pulmonary and Vascular Biology, Department of Pediatrics, University of Texas Southwestern Medical Center, 5323 Harry Hines Blvd., Dallas, Texas 75390-9063, USA. Phone: 214.648.9180; Fax: 214.648.2096; E-mail: Michihisa.Umetani@utsouthwestern.edu.

1. Repa JJ, Mangelsdorf DJ. The liver X receptor gene team: potential new players in atherosclerosis. *Nat Med*. 2002;8(11):1243–1248.
2. Tontonoz P, Mangelsdorf DJ. Liver X receptor signaling pathways in cardiovascular disease. *Mol Endocrinol*. 2003;17(6):985–993.
3. Zelcer N, Tontonoz P. Liver X receptors as integrators of metabolic and inflammatory signaling. *J Clin Invest*. 2006;116(3):607–614.
4. Lu TT, Repa JJ, Mangelsdorf DJ. Orphan nuclear receptors as eLiXiRs and FiXeRs of sterol metabolism. *J Biol Chem*. 2001;276(41):37735–37738.
5. Janowski BA, et al. Structural requirements of ligands for the oxysterol liver X receptors LXRalpha and LXRbeta. *Proc Natl Acad Sci U S A*. 1999;96(1):266–271.
6. Joseph SB, et al. Synthetic LXR ligand inhibits the development of atherosclerosis in mice. *Proc Natl Acad Sci U S A*. 2002;99(11):7604–7609.
7. Terasaka N, et al. T-0901317, a synthetic liver X receptor ligand, inhibits development of atherosclerosis in LDL receptor-deficient mice. *FEBS Lett*. 2003;536(1–3):6–11.
8. van der Hoorn J, et al. Low dose of the liver X receptor agonist, AZ876, reduces atherosclerosis in APOE*3Leiden mice without affecting liver or plasma triglyceride levels. *Br J Pharmacol*. 2011; 162(7):1553–1563.
9. Chawla A, Repa JJ, Evans RM, Mangelsdorf DJ. Nuclear receptors and lipid physiology: opening the X-files. *Science*. 2001;294(5548):1866–1870.
10. Joseph SB, Castrillo A, Laffitte BA, Mangelsdorf DJ, Tontonoz P. Reciprocal regulation of inflammation and lipid metabolism by liver X receptors. *Nat Med*. 2003;9(2):213–219.
11. Blaschke F, et al. Liver X receptor agonists suppress vascular smooth muscle cell proliferation and inhibit neointima formation in balloon-injured rat carotid arteries. *Circ Res*. 2004;95(12):e110–e123.
12. Ross R. Atherosclerosis — an inflammatory disease. *N Engl J Med*. 1999;340(2):115–126.
13. Deroo BJ, Korach KS. Estrogen receptors and human disease. *J Clin Invest*. 2006;116(3):561–570.
14. Mendelsohn ME, Karas RH. The protective effects of estrogen on the cardiovascular system. *N Engl J Med*. 1999;340(23):1801–1811.
15. Marsh MM, Walker VR, Curtiss LK, Banka CL. Protection against atherosclerosis by estrogen is independent of plasma cholesterol levels in LDL receptor-deficient mice. *J Lipid Res*. 1999;40(5):893–900.
16. Hodgin JB, Krege JH, Reddick RL, Korach KS, Smithies O, Maeda N. Estrogen receptor alpha is a major mediator of 17beta-estradiol's atheroprotective effects on lesion size in Apoe$^{-/-}$ mice. *J Clin Invest*. 2001;107(3):333–340.
17. Chambliss KL, Shaul PW. Estrogen modulation of endothelial nitric oxide synthase. *Endocr Rev*. 2002; 23(5):665–686.
18. Chambliss KL, Simon L, Yuhanna IS, Mineo C, Shaul PW. Dissecting the basis of nongenomic acti-

vation of endothelial nitric oxide synthase by estradiol: role of ERalpha domains with known nuclear functions. *Mol Endocrinol*. 2005;19(2):277–289.
19. Chambliss KL, et al. Non-nuclear estrogen receptor alpha signaling promotes cardiovascular protection but not uterine or breast cancer growth in mice. *J Clin Invest*. 2010;120(7):2319–2330.
20. Chambliss KL, et al. Estrogen receptor alpha and endothelial nitric oxide synthase are organized into a functional signaling module in caveolae. *Circ Res*. 2000;87(11):E44–E52.
21. Chambliss KL, Yuhanna IS, Anderson RG, Mendelsohn ME, Shaul PW. ERbeta has nongenomic action in caveolae. *Mol Endocrinol*. 2002; 16(5):938–946.
22. Mouzat K, et al. Absence of nuclear receptors for oxysterols liver X receptor induces ovarian hyperstimulation syndrome in mice. *Endocrinology*. 2009; 150(7):3369–3375.
23. Gong H, et al. Estrogen deprivation and inhibition of breast cancer growth in vivo through activation of the orphan nuclear receptor liver X receptor. *Mol Endocrinol*. 2007;21(8):1781–1790.
24. D'Eon TM, Souza SC, Aronovitz M, Obin MS, Fried SK, Greenberg AS. Estrogen regulation of adiposity and fuel partitioning. Evidence of genomic and non-genomic regulation of lipogenic and oxidative pathways. *J Biol Chem*. 2005;280(43):35983–35991.
25. Krycer JR, Brown AJ. Cross-talk between the androgen receptor and the liver X receptor: implications for cholesterol homeostasis. *J Biol Chem*. 2011; 286(23):20637–20647.
26. Umetani M, et al. 27-Hydroxycholesterol is an endogenous SERM that inhibits the cardiovascular effects of estrogen. *Nat Med*. 2007;13(10):1185–1192.
27. Murugesan G, Sa G, Fox PL. High-density lipoprotein stimulates endothelial cell movement by a mechanism distinct from basic fibroblast growth factor. *Circ Res*. 1994;74(6):1149–1156.
28. Shaul PW. Regulation of endothelial nitric oxide synthase: location, location, location. *Annu Rev Physiol*. 2002;64:749–774.
29. Smart EJ, Ying YS, Mineo C, Anderson RG. A detergent-free method for purifying caveolae membrane from tissue culture cells. *Proc Natl Acad Sci U S A*. 1995;92(22):10104–10108.
30. Cohen AW, Hnasko R, Schubert W, Lisanti MP. Role of caveolae and caveolins in health and disease. *Physiol Rev*. 2004;84(4):1341–1379.
31. Kato S, et al. Activation of the estrogen receptor through phosphorylation by mitogen-activated protein kinase. *Science*. 1995;270(5241):1491–1494.
32. Dutertre M, Smith CL. Ligand-independent interactions of p160/steroid receptor coactivators and CREB-binding protein (CBP) with estrogen receptor-alpha: regulation by phosphorylation sites in the A/B region depends on other receptor domains. *Mol Endocrinol*. 2003;17(7):1296–1314.
33. Maggi A. Liganded and unliganded activation of estrogen receptor and hormone replacement therapies. *Biochim Biophys Acta*. 2011;1812(8):1054–1060.
34. Rubanyi GM, et al. Vascular estrogen receptors and endothelium-derived nitric oxide production in the mouse aorta. Gender difference and effect of estrogen receptor gene disruption. *J Clin Invest*. 1997; 99(10):2429–2437.
35. Razandi M, Pedram A, Levin ER. Estrogen signals to the preservation of endothelial cell form and function. *J Biol Chem*. 2000;275(49):38540–38546.
36. Imayama I, et al. Liver X receptor activator downregulates angiotensin II type 1 receptor expression through dephosphorylation of Sp1. *Hypertension*. 2008;51(6):1631–1636.
37. Shen Q, et al. Liver X receptor-retinoid X receptor (LXR-RXR) heterodimer cistrome reveals coordination of LXR and AP1 signaling in keratinocytes. *J Biol Chem*. 2011;286(16):14554–14563.
38. DuSell CD, Umetani M, Shaul PW, Mangelsdorf DJ, McDonnell DP. 27-hydroxycholesterol is an endogenous selective estrogen receptor modulator. *Mol Endocrinol*. 2008;22(1):65–77.
39. Lannigan DA. Estrogen receptor phosphorylation. *Steroids*. 2003;68(1):1–9.
40. Rochette-Egly C. Nuclear receptors: integration of multiple signalling pathways through phosphorylation. *Cell Signal*. 2003;15(4):355–366.
41. Shiojima I, Walsh K. Role of Akt signaling in vascular homeostasis and angiogenesis. *Circ Res*. 2002; 90(12):1243–1250.
42. Chen J, et al. Akt1 regulates pathological angiogenesis, vascular maturation and permeability in vivo. *Nat Med*. 2005;11(11):1188–1196.
43. Dillon RL, Muller WJ. Distinct biological roles for the akt family in mammary tumor progression. *Cancer Res*. 2010;70(11):4260–4264.
44. Shaul PW. Endothelial nitric oxide synthase, caveolae and the development of atherosclerosis. *J Physiol*. 2003;547(pt 1):21–33.
45. Bischoff ED, et al. Non-redundant roles for LXRα and LXRβ in atherosclerosis susceptibility in low density lipoprotein receptor knockout mice. *J Lipid Res*. 2010;51(5):900–906.
46. Bradley MN, et al. Ligand activation of LXRβ reverses atherosclerosis and cellular cholesterol overload in mice lacking LXRα and apoE. *J Clin Invest*. 2007;117(8):2337–2346.
47. Sundgren NC, et al. Coupling of fcgamma receptor I to fcgamma receptor IIb by SRC kinase mediates C-reactive protein impairment of endothelial function. *Circ Res*. 2011;109(10):1132–1140.
48. Kumar P, et al. Direct Interactions with Gαi and Gβγ mediate nongenomic signaling by estrogen receptor-α. *Mol Endocrinol*. 2007;21(6):1370–1380.
49. Brouchet L, Krust A, Dupont S, Chambon P, Bayard F, Arnal JF. Estradiol accelerates reendothelialization in mouse carotid artery through estrogen receptor-alpha but not estrogen receptor-β. *Circulation*. 2001;103(3):423–428.
50. Seetharam D, et al. High-density lipoprotein promotes endothelial cell migration and reendothelialization via scavenger receptor-B type I. *Circ Res*. 2006; 98(1):63–72.
51. Hewitt SC, Kissling GE, Fieselman KE, Jayes FL, Gerrish KE, Korach KS. Biological and biochemical consequences of global deletion of exon 3 from the ER α gene. *FASEB J*. 2010;24(12):4660–4667.
52. Peet DJ, et al. Cholesterol and bile acid metabolism are impaired in mice lacking the nuclear oxysterol receptor LXRα. *Cell*. 1998;93(5):693–704.
53. Repa JJ, et al. Regulation of absorption and ABC1-mediated efflux of cholesterol by RXR heterodimers. *Science*. 2000;289(5484):1524–1529.